

Impact of the capping layers on lateral confinement in InAs/InP quantum dots for 1.55 μm laser applications studied by magnetophotoluminescence

C. Cornet,^{a)} C. Levallois, P. Caroff, H. Folliot, C. Labbé, J. Even, A. Le Corre, and S. Loualiche

Laboratoire d'Etude des Nanostructures à Semiconducteurs (LENS), CNRS UMR FOTON 6082 INSA, 20 Avenue des Buttes de Coësmes, 35043 Rennes Cedex, France

M. Hayne and V. V. Moshchalkov

Pulsed Field Group, Laboratory of Solid-State Physics and Magnetism, K.U. Leuven, Celestijnenlaan 200D, B-3001 Leuven, Belgium

(Received 30 June 2005; accepted 26 September 2005; published online 30 November 2005)

We have used magnetophotoluminescence to study the impact of different capping layer material combinations (InP, GaInAsP quaternary alloy, or both InP and quaternary alloy) on lateral confinement in InAs/InP quantum dots (QDs) grown on (311)B orientated substrates. Exciton effective masses, Bohr radii, and binding energies are measured for these samples. Conclusions regarding the strength of the lateral confinement in the different samples are supported by photoluminescence at high excitation power. Contrary to theoretical predictions, InAs QDs in quaternary alloy are found to have better confinement properties than InAs/InP QDs. This is attributed to a lack of lateral intermixing with the quaternary alloy, which is present when InP is used to (partially) cap the dots. The implications of the results for reducing the temperature sensitivity of QD lasers are discussed. © 2005 American Institute of Physics.

[DOI: 10.1063/1.2132527]

In the last few years, there has been a great interest in semiconductor nanostructures, and especially quantum dots (QDs).¹ Indeed, the zero-dimensional confinement effect in QDs improves the performance of lasers and wavelength switching devices, and can be used for optical memories.¹ Considering the laser application, such a zero-dimensional confinement is of prime importance in order to guarantee the insensitivity of the device to temperature. Following one of the main quality criteria usually assumed for device temperature insensitivity, the difference between ground-state transition and first-excited-state transition should be larger than $k_b T = 25$ meV at RT. In this regard, physical parameters like exciton Bohr radii, exciton binding energy, and energy differences between ground transition and first excited transitions are well adapted to describe the lateral confinement behavior in QDs.

In order to reach the 1.55 μm (0.8 eV) wavelength used in optical telecommunications, QDs are usually grown on InP substrates.^{2–5} Growth on (311)B oriented substrates leads to good quality QD structures with high densities and low size dispersion. An original double cap method has been developed for controlling the QDs emission energy.⁴ The understanding of the impact of both the first cap layer and the second cap layer on electronic and optical properties is thus crucial for laser applications. Several material combinations have been considered to improve QD laser performance. Using the QDs/1st cap/2nd cap notation, InAs/InP/InP QDs are usually considered as a reference system.^{4,5} But this system has very poor optical confinement and is not suitable for laser applications. InAs/InP/Q1.18 QDs, where Q1.18 is a quaternary alloy $\text{In}_{0.8}\text{Ga}_{0.2}\text{As}_{0.435}\text{P}_{0.565}$ emitting at a wavelength of 1.18 μm , have been used to generate laser

emission.⁶ Recently, InAs/Q1.18/Q1.18 structures have successfully produced laser emission.^{6,7} In this work, we study lateral confinement properties by magnetophotoluminescence^{8,9} and high excitation power luminescence in these three kinds of samples and show that using the quaternary alloy is necessary for the insensitivity to the temperature of QDs lasers emitting at 1.55 μm .

Six samples of single layer InAs/InP/InP (samples A and A'), InAs/InP/Q1.18 (samples B and B') and InAs/Q1.18/Q1.18 (samples C and C') QDs have been grown on an InP (311)B substrate by gas-source molecular beam epitaxy using the Stranski-Krastanov method (Fig. 1). Samples A, B, and C are designed to emit around 0.8 eV at low temperature for magnetophotoluminescence (magneto-PL) experiments.⁴ Samples A', B', and C' are designed to emit around 0.8 eV at RT for high excitation power photoluminescence (PL) experiments.⁴ The sample design is different for the two experiments in order to match the de-

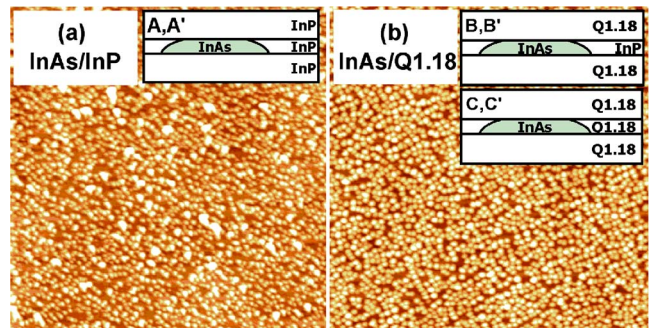


FIG. 1. $2 \times 2 \mu\text{m}^2$ atomic force microscopy pictures of uncapped InAs/InP QDs similar to sample A and A' (a) and uncapped InAs/Q1.18 QDs similar to samples B, B', C, and C' (b). Density and radius are similar in both pictures. The z scale goes from 0 nm (dark areas) to 8 nm (bright areas), which corresponds to the highest dots.

^{a)} Author to whom correspondence should be addressed; electronic mail: charles.cornet@ens.insa-rennes.fr

TABLE I. Lateral confinement parameters for samples A, A', B, B', C, and C'. QD diameters, exciton binding energies, exciton Bohr radii, and energy differences between excited-state and ground-state transitions are presented.

Samples	AFM diameter (nm)	E_{BINDING}^X (meV)	$\sqrt{\langle \rho^2 \rangle}$ (nm)	$\Delta E_1/\Delta E_2$ (meV)
A and A' (InAs/InP/InP)	38	7	7.7	9/24
B and B' (InAs/InP/Q1.18)	36	7	7.8	10/23
C and C' (InAs/Q1.18/Q1.18)	36	12	6.9	26/39

tector spectral bandwidth. In Fig. 1, atomic force microscopy pictures are presented both for uncapped InAs QDs on InP (similar to sample A and A') and InAs QDs on Q1.18 (similar to samples B, B', C, and C'). From these pictures, a comparison can be made between these two kinds of QDs. Densities are found to be $5.8 \times 10^{10} \text{ cm}^{-2}$ on InP sample, and $6.1 \times 10^{10} \text{ cm}^{-2}$ on the Q1.18 sample. Dot radii are unchanged from one sample to another, equal to about $(18 \pm 3) \text{ nm}$ for Q1.18 and $(19 \pm 4) \text{ nm}$ for InP. These values are reported in Table I. The similarity between these two samples allows us to interpret any further differences between samples A, B, and C as a consequence of the capping procedure and/or confinement induced by the barrier materials.

Magneto-PL experiments are carried out at 4.2 K in a He bath cryostat placed in the bore of a pulsed magnet with a maximum field of 50 T.^{10,11} The field is applied parallel to the growth direction (z). A single 550 μm core optical fiber is used to collect the PL signal, which is excited by the light from a cw frequency-doubled Nd:yttrium-aluminium-garnet (YAG) laser at 532 nm via a second fiber. A cooled InGaAs linear diode array coupled to an optical spectrum analyzer is used to detect the PL. The impact of a magnetic field on QDs samples has been already studied.^{8,10} Following this excitonic model, at zero and low magnetic fields, the electron and hole within the dot are strongly spatially confined by the physical boundaries of the dot. In these conditions, magnetic field can be treated as a perturbation in the Hamiltonian, leading to a square dependence of the energy shift on the magnetic field: $\Delta E = e^2 \langle \rho^2 \rangle B^2 / 8\mu_r$,^{8,10} for $B < B_c = 2\hbar / e \langle \rho^2 \rangle$ where $\sqrt{\langle \rho^2 \rangle}$ is the in-plane effective exciton radius (Bohr radius), μ_r is the in-plane exciton effective mass, B is the magnetic field, and B_c is the crossover magnetic field, which depends only on $\sqrt{\langle \rho^2 \rangle}$. At sufficiently high field ($B > B_c$), when the attempted Larmor radius is smaller than the spatial size of the dot, the charges become confined by the field in the plane perpendicular to the applied field, and the energy levels shift linearly with B : $\Delta E = \hbar e B / 2\mu_r$.^{8,10} Using this expression, measurements can be fitted with only two free parameters: the effective mass and the Bohr exciton radius. Consequently, the exciton binding energy is given by: $E_{\text{BINDING}}^X = \hbar^2 / 2\mu_r \langle \rho^2 \rangle$.

This analysis has been performed on data from the three samples. Values for exciton Bohr radii and exciton binding energies are presented in Table I. Figure 2 represents the evolution of photoluminescence for samples B and C as a function of B^2 . The dotted line represents the extrapolation of the linear fit for sample C in the $[0; 713 \text{ T}^2]$ range. It is clear that both curves deviate from a linear B^2 dependence. The

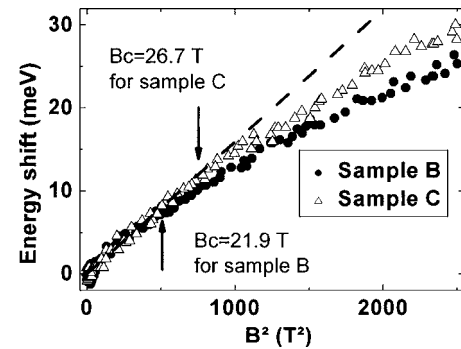


FIG. 2. Magnetophotoluminescence measurements for samples B and C. Evolution of ground-state transition peaks is plotted as a function of the square of the magnetic field. The dashed line is the extrapolation of a linear fit for sample C between 0 and 713 T². The influence of the first capping layer composition on lateral confinement is shown by the field at which the data deviate from a straight line.

field at which this deviation occurs depends only on $\sqrt{\langle \rho^2 \rangle}$, thus it can immediately be seen that the lateral spatial extent of the wavefunction is smaller in sample C than in sample B and in sample A (see also Table I). From these data we see that the first capping layer is of prime importance for the lateral confinement, which is increased by using Q1.18 instead of InP in the first capping layer. This finding is further corroborated by the exciton binding energy, which is 70% larger for sample C than for samples A and B. The observation of enhanced confinement with Q1.118 as a first cap layer is, however, not consistent with published theory. Parameters like E_{BINDING}^X , $\sqrt{\langle \rho^2 \rangle}$, or μ_r , representing the lowest limit for electronic effective mass, have been studied in previous works.¹²⁻¹⁴ InP has a larger band gap than Q1.18, which should lead to better lateral confinement, i.e., a larger E_{BINDING}^X and a smaller $\sqrt{\langle \rho^2 \rangle}$. Thus the difference in confinement between the samples cannot be explained by the intrinsic nature of the barrier material, but is a consequence of the growth procedure. Moreover, we have demonstrated that the difference appears when the first capping layer composition changes. The strength of the lateral confinement potential is linked to two parameters: the height of the confinement barrier, and the spatial extent of the confinement potential. While the total height of the confinement barrier cannot be changed, the spatial extent of the confinement potential is not fixed during the growth. Lateral diffusion of atoms during the growth leads to a spatial gradient of composition and confinement potential. Several growth phenomena are based on this mechanism, such as indium segregation, demixing or intermixing.¹⁵ When we compare our results with the calculations,¹²⁻¹⁴ a larger difference is noticed for InP samples between theory and experiment than for Q1.18 sample. Indeed, these calculations did not take into account any growth effect during the capping procedure. Considering that P₂ growth interruption enhances the As/P exchange during the growth (after first cap deposition),⁴ we propose to interpret the difference between experiment and calculations as a result of a lateral intermixing effect between InAs and the InP first capping layer, during the double cap procedure. This intermixing effect leads to a composition gradient in the lateral plane, reducing the lateral confinement in InP based samples (A and B). This effect is lower with a Q1.18 first capping layer. Therefore, sample C has a better lateral confinement than samples A and B. In order to study the conse-

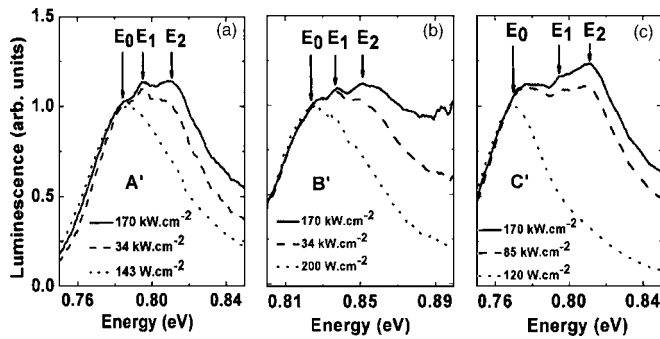


FIG. 3. High excitation power PL measurements for samples A', B', and C' at room temperature for (a) InAs/InP/InP sample with excited-state transitions at $E_1 = E_0 + 9$ meV and $E_2 = E_0 + 24$ meV. (b) InAs/InP/Q1.18 sample with excited-state transitions at $E_1 = E_0 + 10$ meV and $E_2 = E_0 + 23$ meV. (c) InAs/Q1.18/Q1.18 sample with excited-state transitions at $E_1 = E_0 + 26$ meV and $E_2 = E_0 + 39$ meV.

quences of such a difference on spectral and electronic properties, high power photoluminescence experiments are performed on similar samples.

High power PL experiments are carried out at RT. The luminescence is excited with a YAG laser at $1.06 \mu\text{m}$ focused on the sample with a microscope objective, leading to a maximum excitation power of 170 kW cm^{-2} . An InGaAs detector is used, coupled to an optical spectrum analyzer. Figure 3 represents luminescence spectra for samples A', B', and C'. Luminescence is performed for various excitation powers, so that excited-state transitions can be seen easily. Measured differences between ground and excited state transitions are reported in Table I. Consequently, sample C' seems to be very different from samples A' and B'. The link between the distance of the excited transition to the ground transition and the lateral confinement has already been shown previously.¹⁶ The stronger the lateral confinement is, the farther the excited-state transitions are from ground-state transitions. In this regard, the InAs/Q1.18/Q1.18 samples are confirmed as the strongest confining structures.

These spectral considerations are of direct relevance to laser applications. One of the main quality criteria usually assumed for device temperature insensitivity is given by ΔE_1 and $\Delta E_2 > k_B T = 25$ meV at RT. In this respect, samples A and B with a first capping layer of InP are not suitable for laser applications while sample C, with a first capping layer of Q1.18, is convenient in order to develop temperature insensitive lasers. Moreover, samples C and C' have better optical confinement, leading to better carrier injection.⁶ Insensitivity to the temperature of QDs lasers could perhaps be further improved, by using other materials, or by changing the shape of the QDs and especially their aspect ratio. We should keep in mind that, in order to have a good quality QD laser, we also need a low threshold current density. In such a Q1.18 system, high QDs density can be reached,¹⁷ leading to low threshold current density lasers.^{6,7} Thus, the InAs/Q1.18/Q1.18 QD system, appears to achieve both low threshold current densities and insensitivity to temperature, which are two of the major performance criteria for (QD) lasers.

In conclusion, InAs/InP/InP QDs, InAs/InP/Q1.18 QDs, and InAs/Q1.18/Q1.18 QDs were studied by magneto-PL and high excitation power PL. On the first two structures, the lateral confinement is weakened, which is interpreted as a consequence of enhanced lateral intermixing during growth. These electronic properties make such structures unsuitable for laser applications. On the other hand, measurements show that InAs/Q1.18/Q1.18 QDs have a very different electronic and optical signature. The influence of the first capping layer is thereby demonstrated, and a weak lateral intermixing for InAs/Q1.18/Q1.18 QDs is considered to be responsible for the improved confinement. Moreover, a high QD density has already been reached in this system, as required for low threshold current density lasers. In these regards, the choice of InAs/Q1.18/Q1.18 QDs seems to be at present the best in this system for achieving QDs lasers emitting at $1.55 \mu\text{m}$ with low threshold density currents, and large insensitivity to the temperature.

This work was supported by the EuroMagNET project (Contract No. R113-CT-2004-506239) and the SANDiE Network of Excellence (Contract No. NMP4-CT-2004-500101) of the 6th Framework Programme of the European Commission.

- ¹D. Bimberg, M. Grundmann, and N. N. Ledentsov, *Quantum Dot Heterostructures* (Wiley, Chichester, 1999).
- ²S. Frechengués, N. Bertru, V. Drouot, B. Lambert, S. Robinet, S. Loualiche, D. Lacombe, and A. Ponchet, *Appl. Phys. Lett.* **74**, 3356 (1999).
- ³C. Paranthoën, N. Bertru, B. Lambert, O. Dehaese, A. Le Corre, J. Even, S. Loualiche, F. Lissillour, G. Moreau, and J. C. Simon, *Semicond. Sci. Technol.* **17**, L5 (2002).
- ⁴C. Paranthoën, C. Platz, G. Moreau, N. Bertru, O. Dehaese, A. Le Corre, P. Miska, J. Even, H. Folliot, C. Labbé, G. Patriarche, J. C. Simon, and S. Loualiche, *J. Cryst. Growth* **251**, 230 (2003).
- ⁵C. Cornet, C. Labbé, H. Folliot, N. Bertru, O. Dehaese, J. Even, A. Le Corre, C. Paranthoën, C. Platz, and S. Loualiche, *Appl. Phys. Lett.* **85**, 5685 (2004).
- ⁶C. Platz, C. Paranthoën, P. Caroff, N. Bertru, C. Labbé, J. Even, O. Dehaese, H. Folliot, A. Le Corre, S. Loualiche, G. Moreau, J. C. Simon, and A. Ramdane, *Semicond. Sci. Technol.* **20**, 459 (2005).
- ⁷P. Caroff, C. Platz, O. Dehaese, C. Paranthoën, N. Bertru, A. Le Corre, and S. Loualiche, *J. Cryst. Growth* **278**, 329 (2005).
- ⁸M. Hayne, J. Maes, S. Bersier, M. Henini, L. Müller-Kirsch, R. Heitz, D. Bimberg, and V. V. Moshchalkov, *Physica B* **346**, 421 (2004).
- ⁹S. Raymond, S. Studenikin, S. J. Cheng, M. Pioro-Ladrière, M. Ciorga, P. J. Poole, and M. D. Robertson, *Semicond. Sci. Technol.* **18**, 385 (2003).
- ¹⁰M. Hayne, R. Provoost, M. K. Zundel, Y. M. Manz, K. Eberl, and V. V. Moshchalkov, *Phys. Rev. B* **62**, 10324 (2000).
- ¹¹J. Maes, M. Hayne, Y. Sidor, B. Partoens, F. M. Peeters, Y. Gonzalez, L. Gonzalez, D. Fuster, J. M. Garcia, and V. V. Moshchalkov, *Phys. Rev. B* **70**, 155311 (2004).
- ¹²H. Folliot, S. Loualiche, B. Lambert, V. Drouot, and A. Le Corre, *Phys. Rev. B* **58**, 10700 (1998).
- ¹³P. Miska, C. Paranthoën, J. Even, N. Bertru, A. Le Corre, and O. Dehaese, *J. Phys.: Condens. Matter* **14**, 12301 (2002).
- ¹⁴P. Miska, J. Even, C. Paranthoën, O. Dehaese, H. Folliot, S. Loualiche, M. Senes, and X. Marie, *Physica E (Amsterdam)* **17**, 56 (2003).
- ¹⁵D. M. Bruls, J. W. A. M. Vugs, P. M. Koenraad, H. W. M. Salemink, J. H. Wolter, M. Hopkinson, M. S. Skolnick, F. Long, and S. P. A. Gill, *Appl. Phys. Lett.* **81**, 1708 (2002).
- ¹⁶K. H. Schmidt, G. Medeiros-Ribeiro, J. Garcia, and P. M. Petroff, *Appl. Phys. Lett.* **70**, 1727 (1997).
- ¹⁷C. Cornet, C. Platz, P. Caroff, J. Even, C. Labbé, H. Folliot, A. Le Corre, and S. Loualiche, *Phys. Rev. B* **72**, 035342 (2005).